

Miniature Optical Joint Measurement Sensor for Robotic Application Using Curvature Based Reflecting Surfaces

Dalia Osman¹, Wanlin Li², Xinli Du¹, Timothy Minton¹, Yohan Noh^{1*}

¹ Dept. of Mechanical and Aerospace Engineering, Brunel University London, United Kingdom

² Centre for Advanced Robotics @ Queen Mary (ARQ), Queen Mary University London, United Kingdom

* IEEE Member

Manuscript received February 24, 2022;

Abstract— The miniaturization of robotic applications such as flexible manipulators or robotic prosthetics while maintaining high-precision closed-loop position control faces the challenge of integrating all their mechanisms, sensors, and actuators within a limited space. For this reason, position sensors are usually installed outside the actuated joints, by for example using a wire (tendon)-driven system. In this case, high-precision position control may not be guaranteed due to wire slack or wire deformation caused by high tension. As such, this paper presents an optoelectronic based joint measurement sensor capable of not only being integrated directly within joints of a versatile range of robotic applications, but also enhancing further miniaturization of these robot applications. Using a variable thickness reflecting surface for proximity-based intensity modulation, the proposed sensing system is shown to be able to measure a larger angular range of $[0-140^\circ]$, with increased sensitivity (0-3.5 V) along with investigation of a light intensity model for estimation of sensor output.

Index Terms — position sensing, optoelectronic sensor, optic technology, angle measurement sensor.

I. INTRODUCTION

Joint measurement sensors within robotic applications are a crucial element of accurate, safe, and stable position feedback control. When considering applications such as robotic prosthetics or soft robotics in MIS (Minimally Invasive Surgery), which differ in motion compared to more traditional rigid robots in terms of flexibility, integration of these sensors in a way that will not obstruct or reduce required motion is vital. This is one of the challenging aspects encountered when introducing sensing with such applications, and a sensing solution that offers miniaturized features while also allowing sufficient angular sensing range with necessary sensitivity is a further challenge that must be addressed. While traditional rigid robots such as industrial robotic arms use joint position sensors such as magnetic and optical encoders that are incredibly accurate, this does not translate well to the mentioned applications such as soft continuum robots as their large size can occupy a substantial amount of space. These encoders are typically mounted within the joints and can measure joint motion directly by generating a high to low voltage signal as they rotate, using a pattern of slits or magnetized poles. Although sizing down is possible, this comes at a cost of lower resolution and accuracy. Many robotic devices overcome this size issue by using encoders and other sensors such as potentiometers externally rather than at the joint, for example using tendon-length based mechanism measurements [1]. However, when considering high tension that causes deformation, or slack of the tendon wires by the lack of tension, uncertainties can arise and lead to loss in accuracy when estimating joint position in this way. Therefore, this is not considered a feasible solution, and use of sensors directly at joint locations remains a more suitable way to ensure highest accuracy of measuring joint position. In many robotic devices

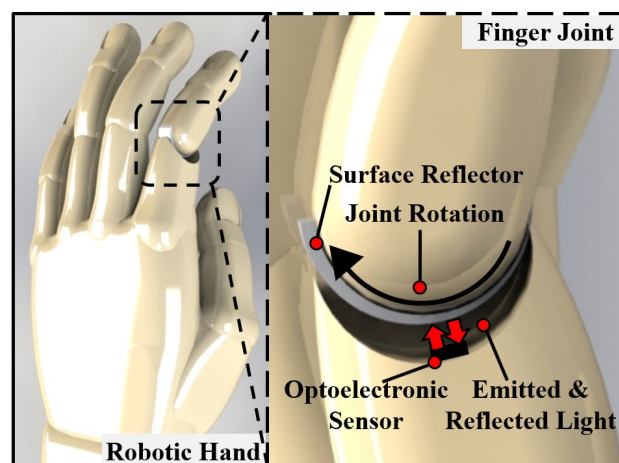


Figure 1: (Left) Concept image for light intensity modulated sensing for finger joints of robotic hand (adapted from GrabCad, J.Schmit, 2012). (Right) The sensor is integrated within one joint opposing a reflective surface on the coupled joint. Variable thickness of reflective surface modulates light intensity due to proximity difference when the joint angle changes due to motion.

such as soft continuum robots, robotic hands or haptic gloves that consist of smaller joints, it is the miniaturization of sensing systems that allow the integration directly within the joint. Many types of miniaturized sensing systems have been proposed for joint measurement. A common choice of sensor used within robotic applications is the use of MEMS (Micro electro-mechanical) sensors; an example is an inertial sensor [2]. These can measure position and orientations and comprise of accelerometers, magnetometers, and gyroscopes. One disadvantage is that these small elements have been reported to suffer from increased error in position estimation due to both gyroscopic drift as well as error from vibrations during fast motion and magnetic interference. Another sensing techniques shown in [3] uses a thin flexible film that has sensing elements with microchannels filled with conductive liquid. Deformation or bending

Corresponding author: Yohan Noh (e-mail: Yohan.noh@brunel.ac.uk).
Associate Editor:

Object Identifier

of the microchannels leads to a change in electrical resistance and can therefore detect changes in angle when applied to a robotic hand. Results showed measurement of up to 90° with relatively large estimation errors after calibration. Use of mentioned conductive liquid may also not be suitable for certain applications, such as MIS based robotics, due to the irritant and toxic properties when in contact with the human body. Many similar types of stretch or film sensors have been proposed, although are complex to manufacture, and inhomogeneity of material and electrical properties through the sensor can lead to error. Many alternative optical based sensors have also been proposed. For example [4] shows the use of optoelectronic sensors to measure pose in the exoskeleton of a robotic hand actuator. Optoelectronic sensors comprise of a Light Emitting Diode (LED) that emits infrared light and a Phototransistor (PT) to collect reflected light. A chain of these sensors were fitted into a flexible multisegmented unit. By using the back of each sensor segment as a reflective surface, light emitted from the LED is reflected, of which signals are captured by the phototransistor. Through this modulation of light intensity, the signals are converted to joint angle estimations, and using the measured angle between each consecutive unit, these would summate to give the overall angle of the joint. Results showed sensor measurement up to 90° , with sensor sensitivity of 0.047 V° , however this required 5 sensors to measure this range, where despite the sensor categorizing as miniature, the configuration required for the sensing system is enlarged, and can become bulky when considering more than one joint. Palli et al demonstrated an optical based joint measurement sensor for a tendon driven robotic hand using an LED and a Phototransistor component [5]. These components were placed in the joint between which a variable thickness canal was positioned. As the joint moved, the canal thickness varied the amount of light able to transmit across from the LED to the Phototransistor. This modulation of light allowed a joint angle sensor to be developed, and results have shown a sensor measurement range of $0\text{-}110^\circ$ over almost 2.5 V sensor output, although requires two separate sensing elements that makes this harder to further miniaturize the sensing system. Previous work in [6] shows the use of a single optoelectronic unit (*QRE1113 ON Semiconductor Reflective Sensor*) used to measure joint angle in applications such as a soft robotic joint. A prototype was used, comprising of two links coupled with a rotational joint. With the sensor mounted on one link face, the opposing coupled link face was utilized as a flat reflective surface. This offered a more miniaturized sensing configuration than the two previous configurations, with only one coupled sensor being used against a single reflective surface. Similarly, however, using the modulation of light intensity through the proximity change between the sensor and a reflective surface during motion, signals were recorded and used to estimate joint angle. However due to the particular placement of the sensing unit and flat reflective surface, results showed a small sensing range of just $0\text{-}40^\circ$. The optoelectronic methods discussed above are advantageous due to components being miniature, easily able to integrate directly at joints, with low cost and low noise. However, considering the inverse relationship between light and radial distance as it propagates, the disadvantage of these sensors is that output can present a non-linear response. At further distances between the sensor and reflector, signal value can saturate due to this property, meaning that less of the signal range can be used, and sensor resolution can be lower. This is not ideal, and higher sensor resolution is desired as it can increase sensing accuracy and provide more stable control when implemented into position feedback of a robotic control system. Therefore, this paper introduces an optoelectronic proximity-based sensor for measuring joint angles, as an extension of previous work. Using a curved surface reflector of variable thickness that can fit axially on a joint, with a sensor fit on a coupled joint, it can be shown that resolution and

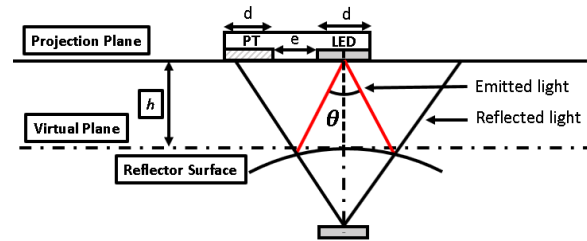


Figure 2: Light is emitted from LED ($d = 0.4\text{mm}$) with beam angle ($\theta = 50^\circ$) onto a curved reflector. Modelling of a virtual LED source on a virtual plane to find path of reflected light to projection plane is used.

angular sensing range of the sensor can be varied, for improved sensor performance. The proposed sensing principle is demonstrated in the concept image in Fig 1 that shows the sensing configuration implemented into the finger joint of a robotic hand. With the sensor fixed on one joint and coupled to a rotating joint where the reflector is mounted, light can be variably reflected and received by the phototransistor. This is by varying the curve of this surface through the change in thickness around the reflector, which leads to the change in proximity of the surface to the sensor to give the varying signal output. With this modulation in light intensity, calibration can then be used to develop a joint angle sensor. The miniature dimensions of the chosen sensor - the NJL5901R-2 (New Japan Radio Photodetector, $1 \times 1.4 \times 0.6 \text{ mm}$) and reflector allows for a reduction of space taken, while the short distance range responsivity of the sensor ($0\text{-}2 \text{ mm}$) further reduces the space required between sensor and reflector, compared to a previously used sensor QRE1113, to give a more compact design which would make this suitable for a range of different robotic applications including soft robotics. The sensor exhibits ideal properties such as low noise, high voltage variation (over a short displacement range) for increased resolution, no signal disturbance due to external interference, and offers a significantly reduced cost of materials and simple fabrication. Based on this principle, the proposed optoelectronic joint sensing system aims to increase the sensor sensitivity and sensing range. This will be done through testing a range of reflective surfaces that vary in curvature, and the effect this has on the sensor output will be studied through experimental results as well as through mathematical modelling, using a light intensity model to estimate theoretical light intensity output.

II. THEORETICAL BACKGROUND

A. Light Intensity Model

As described, the sensing principle is based on the modulation of emitted and reflected light intensity. Using a previously evaluated light intensity model [6], the behaviour of the sensor under certain geometrical conditions can be studied. It is assumed that the light emits conically from the LED with a gaussian distribution. The intensity model listed in [6] is used to estimate sensor output based on light reflected from a surface that rotates with varying angle φ . Under current construction of the sensor configuration, the value of φ is set to zero, as the sensor is placed opposite the reflective surface, as in Fig 2. Despite the curved surface, this is assumed to be flat due to the low curvature compared to the sensor size. The flux (ϕ_c) collected by the PT can then be calculated as in Eq 1, by integrating the initial light intensity distribution with boundaries of the LED and phototransistor structures over the conically formed projection on the projection plane. Here, h represents the varying distance between the sensor and the reflector surface, which changes as the joint rotates about a vertical axis, d is the LED diameter, θ is the LED beam angle, and ϵ is the distance between the PT and LED. Finally, a^2 represent the conical

beam width. This flux can then be converted to a theoretical voltage value by multiplying by a conversion factor k_v and reflectance rate R , as in Eq 2.

$$\phi_c = \int_{-\frac{1}{2}d-\epsilon}^{-\frac{1}{2}d+\epsilon} \int_{-\sqrt{\left(\frac{d}{2}\right)^2 - (y-h\tan(\theta)+d+\epsilon)^2}}^{\sqrt{\left(\frac{d}{2}\right)^2 - (y-h\tan(\theta)+d+\epsilon)^2}} I_0 e^{-2\left(\frac{x^2+y^2}{a^2}\right)} dy dx \quad (1)$$

$$V_{th} = \phi_c \cdot R \cdot k_v \quad (2)$$

B. Curved Reflector Design

As previously described, a curved reflective surface was designed with the aim of achieving a larger sensing range compared to previous attempts that utilized flat reflective surfaces. The Figure 3 graph supplied by the datasheet of the sensor (NJL5901R-2) shows the response with linear displacement to a reflective aluminium evaporation surface under ideal test conditions [7]. Based on this data, a usable sensor range can be selected. A generally linear range between 0.3 – 1 mm is seen, with a less sloped response beyond this distance as it plateaus. From this data, the 0.3-2.3 mm sensing range is used as the starting point for the design of the reflective curved surfaces, as highlighted in yellow colour. As shown in Fig 4b, the designed surface curves around a circular path. The top of the part consists of screw holes that may be fixed to the motor horn of the experimental set up (Fig 4a). Starting on one end, the thickness of the curve is 3 mm, and this gradually decreases to a thickness of 1 mm, therefore reducing by 2 mm in total over a certain angle range (α) around the circular path, in order to coincide with the range selected from the data sheet. With this gradual change in curvature, an assumption is made as described in the model in section II that the point at which light reflects on the surface is taken to be flat.

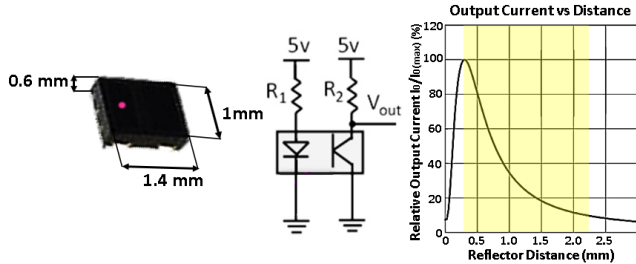


Figure 3: (Left) NJL5901R-2 sensor dimensions and electrical component make up. LED resistance R_1 and PT resistance R_2 are set to 1 k Ω and 10 k Ω respectively. (Right) Datasheet graph shows sensor displacement response under ideal conditions

III. MATERIALS AND METHODS

A. Experimental Set Up

To study the sensor response with varying reflective surfaces, the experimental setup was constructed as in Figure 4a. A DC Servo Motor (Dynamixel XL430-W-250T, ROBOTIS, South Korea) was used to generate the joint motion, and on it was fixed a motor horn component. The fixed upper component was rotationally coupled to the motor using a bearing within the motor horn. On this fixed component, the optoelectronic sensor is mounted into place. The components were 3D printed using PLA (Polylactic acid) plastic, other than the interchangeable curved slopes to be tested, which were designed, and 3D printed using a high-resolution resin printer so that the surface finish was as smooth as possible. The curved edge of the surfaces were covered with reflective aluminium tape in order to maximize reflectance rate. These were screwed onto the motor horn component to move together with the motor. The sensor was wired to

an Arduino Mega ADK board (5 V) and connected to the PC. 12 V power was supplied to the motor, which was connected to a U2D2 communication device also connected to the PC. Python software was

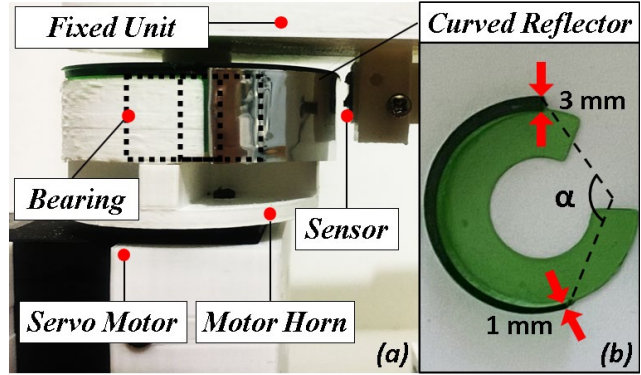


Figure 4: (a) Experimental Set Up – Curved reflector component is fixed onto the rotating motor horn that is attached to a servo motor. The sensor is mounted onto the fixed upper component that is coupled to the motor horn with a bearing (b) Reflector surface design parameters

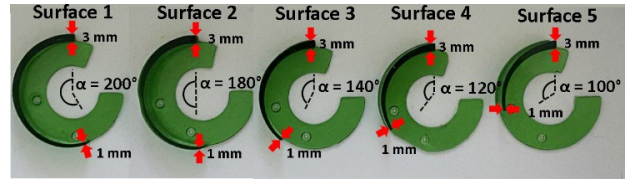


Figure 5: Bottom section view of the design of Surfaces (1-5) showing curvature change over range of α values.

used to synchronously interface the motor encoder position as it was commanded to rotate for a given angular range, along with the analogue sensor values. This data was recorded and stored through each of the experiments. With each curved surface that was tested, the thickness of the curved structure was varied by changing the angular range (α) over which the thickness ranged from 3-1 mm, as depicted in Fig 3 (Right). The initial disk tested had the thickness range descend over $\alpha = 200^\circ$. Subsequent curved surfaces tested were over $\alpha = 180^\circ$, 140° , 120° and 100° . These are shown in Fig 5, labelled Surfaces 1-5. Fig 6 in Section IV shows the results of each of the tested surfaces that essentially change in curvature, and the effect this has on the sensor output over an angular range of motion of the experimental joint, while also comparing to the theoretical output predicted by the light intensity model described prior in Section II, and this is discussed in the Discussion section.

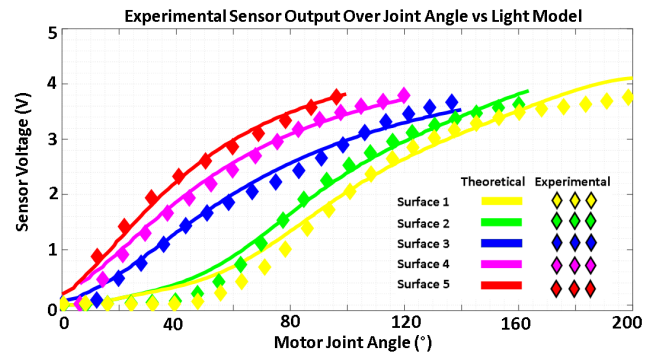


Figure 6: Results showing the sensor voltage output over a joint angle range with different curvature surfaces collected during experiments (dotted). Each output curve is compared to the theoretical output based on the light model.

IV. RESULTS and DISCUSSION

TABLE I. Experimental vs Theoretical sensor output

	PERCENTAGE ERROR (%)	RMSE (°)
Surface 1	56.36	0.44
Surface 2	27.97	0.22
Surface 3	14.38	0.19
Surface 4	8.35	0.15
Surface 5	8.72	0.17

Figure 6 shows the sensor output over the angular motion range of the servo motor based on the motor encoder data, with different reflective surfaces used of varying curvatures, as shown with the dotted lines. As seen for Surface 5 ($\alpha = 100^\circ$), which changes through the thickness range (3-1 mm) over 100° , therefore having the highest curvature, the sensor output shows a high voltage variation. The voltage level increases from around 0 V to 4 V. Voltage variation decreases in looking at subsequent surfaces, such as surface 4 ($\alpha = 120^\circ$) and 3 ($\alpha = 140^\circ$), although show a longer angular sensing range, with the graph starting to plateau at later point. This is due to the signal starting to reach a saturation point as the maximum distance of the reflector to sensor is reached, where steeper curves reach this point earlier in the angle range. Surfaces 2 ($\alpha = 180^\circ$) and 1 ($\alpha = 200^\circ$) on the other hand show the lowest voltage variation. Unlike prior tested surfaces, the initial increase of the graph is slower, likely due to a slower change in distance between sensor and reflector as the motor rotated, owing to the lower curvature. Comparing to the experimental data (dotted) is the theoretical output (solid line) for each of the surfaces, based on the equations describing the light model in Section II. The theoretical curves generated by the model show a good fit to the experimental data, which appears to follow the trend set by this predicted model data. Table I shows both percentage error and Root Mean Square Error (RMSE) between the experimental and theoretical data. Surface 5 ($\alpha = 100^\circ$) having a larger curvature shows the lowest error, while the largest error is seen for Surface 1 ($\alpha = 200^\circ$), having the lower curvature. As some assumptions were made to simplify the model, such as assuming the surface was flat despite the designed curvature, this may have been the reason for some deviation between the experimental data and the theoretical values. It is possible that in the lower curvature surfaces that were tested, more reflected light was directed towards the sensor in terms of scattering, as these surfaces were flatter compared to high curvature surfaces. Another general reason may have also been that although steps were taken to design a smooth surface with a highly reflective face, this may not have been as fully reflective as in the ideal case shown by the model. A resin 3D printer was used to fabricate the surfaces; however, some unevenness may have remained, which could have led to more scattering or the source of some noise in the data, adding to some mismatch between the experimental and theoretical data. Alternatively, this may have been due to some vibration in the motor during rotation. To improve upon these aspects, steps can be taken to create more ideal experimental conditions, such as better fabrication of the reflective surface, for example by the use of an aluminium evaporation technique. Experimental set ups and subsequent prototypes should be shielded from external ambient light to account for any background noise. Although these steps can be taken to improve results, it can be said however that the approach shows the basis of developing a simple joint angle sensor. The curved surface structure can be said to have increased the sensing range, for example as seen for surface 3 ($\alpha = 140^\circ$), that has a fully usable sensing range of 0° up to 140° . This is an improvement when considering previous attempts using a flat reflecting surface as shown in [6], as well as previous work listed in the Section I. It shows a voltage variation of around 3.5 V, which

again is an improvement from previous studies, and the principle of varying curvature of the reflectors to increase this voltage variation can be utilized depending on the required angular sensing range by the user. This is ideal as it allows the increase of sensor sensitivity, or resolution, and therefore accuracy to be achieved as required.

V. CONCLUSION

In conclusion, a simple basis of a joint measurement sensor has been developed and initial experiments show capability for increasing sensing accuracy through increased sensitivity as well as increased sensing range through the use of a curved reflecting surface configuration. The sensor system is miniature, low cost, and easy to integrate into a variety of robotic systems, including soft robotics, for a multitude of applications. Future steps will include the further development of the light intensity model, and through more advanced fabrication techniques, a more specialized prototype for directed robotic application can be developed and tested.

ACKNOWLEDGMENT

The research leading to these results has received funding from EPSRC DTP, Department of Mechanical and Aerospace Engineering, Brunel University London.

REFERENCES

- [1] W. Quan, H. Wang, and D. Liu, "A Multifunctional Joint Angle Sensor with Measurement Adaptability," November, 2013, doi: 10.3390/s131115274.
- [2] Z. Zhang, J. Shang, C. Seneci, and G. Z. Yang, "Snake robot shape sensing using micro-inertial sensors," IEEE International Conference on Intelligent Robots and Systems, pp. 831–836, 2013, doi: 10.1109/IROS.2013.6696447.
- [3] R. K. Kramer, C. Majidi, R. Sahai, and R. J. Wood, "Soft Curvature Sensors for Joint Angle Proprioception," pp. 1919–1926, 2011, doi: 10.1109/IROS.2011.6094701.
- [4] Bo He, Min Li, Renghao Liang, Ziting Liang, Wei Yao, Sina Sareh, Jun Xie, Guanghua Xu, and Yohan Noh, "Optoelectronic-based pose sensing for a hand rehabilitation exoskeleton continuous structure, IEEE Sensors Journal, 2022, doi: 10.1109/JSEN.2022.3147227
- [5] G. Palli and S. Pirozzi, "An optical joint position sensor for anthropomorphic robot hands," Proceedings - IEEE International Conference on Robotics and Automation, pp. 2765–2770, 2013, doi: 10.1109/ICRA.2013.6630958.
- [6] D. Osman, X. Du, W. Li, and Y. Noh, "An Optical Joint Angle Measurement Sensor based on an Optoelectronic Sensor for Robot Manipulators," in 2020 8th International Conference on Control, Mechatronics and Automation, ICCMA 2020, Nov. 2020, pp. 28–32. doi: 10.1109/ICCMAS1325.2020.9301526.
- [7] Y. Noh, S. Han, P. Gawenda, W. Li, S. Sareh, and K. Rhode, "A Contact Force Sensor Based on S-Shaped Beams and Optoelectronic Sensors for Flexible Manipulators for Minimally Invasive Surgery (MIS)," IEEE Sensors Journal, vol. 20, no. 7, pp. 3487–3495, 2020, doi: 10.1109/JSEN.2019.2945163